From epidemics to information propagation: Striking differences in structurally similar adaptive network models

Stojan Trajanovski,[1,*] Dongchao Guo,[2,†] and Piet Van Mieghem[1]

[1] *Faculty of Electrical Engineering, Mathematics and Computer Science, Delft University of Technology, P. O. Box 5031, 2600 GA Delft, The Netherlands*

[2] *Big Data and Network Engineering Research Center, RIIT, Tsinghua University, Beijing, P. R. China*

(Dated: September 16, 2015)

The continuous-time Susceptible-Infected-Susceptible (SIS) epidemic model (ASIS) and the adaptive information diffusion (AID) are two adaptive spreading processes on networks, in which a link in the network changes depending on the infectious state of its end-nodes, but in opposite ways: (1) In ASIS, a link is removed between two nodes if exactly one of the nodes is infected to suppress the epidemic, while a link is created in AID to speed up the information diffusion; (2) A link is created between two susceptible nodes in ASIS to strengthen the "healthy part" of the network, while a link is broken in AID due to the lack of interest in information-less nodes.

ASIS and AID may be considered as first-order models for cascades in real-world networks. While the ASIS model has been exploited in the literature, we show that the AID model is realistic by obtaining a good fit with Facebook data. Contrarily to the common belief and intuition for such similar models, we show that ASIS and AID exhibit different, but not opposite properties. Most remarkably, a unique metastable state always exists in ASIS, while there are "sand-clock shaped" region of instability in AID. Moreover, the epidemic threshold is a linear function in the effective link-breaking rate in AID, while it is almost constant but noisy in the AID model.

PACS numbers: 89.75.Hc, 87.10.Ed, 89.75.Fb

Over the last decade, many real-world networks have been characterized via graph metrics [1–3] such as clustering, assortativity, modularity, degree distribution and spectral properties. Recently, robustness characteristics and complex dependencies have been analyzed in networks of networks [4], while a parallel track in network science focuses on relatively simple dynamic processes on networks such as epidemics [5, 6], synchronization [7] and opinion diffusion [8–10]. In most studies so far, the networks are considered fixed or independent of the dynamic process. After the seminal work of Gross *et al.* [11], the coupling between epidemic processes and the underlying network topology has been extensively studied [12–15].

The coupling between process and topology is natural in many cases. In epidemics [16], for example, after the observation of an infectious relative, one may either avoid him/her (by changing the social contact network) or increase the protection against the virus (without altering the topology). In human brain networks, Hebbian learning alters the connectivity between brain regions that are trained or neurally excited. Although self-adaptation naturally occurs in biology, adaptive networks, in which the process interacts with the topology, are unfortunately difficult to analyze and we barely understand the interplay between process and topology. Twitter measurements [17, 18] show that the topology of the network adaptively changes connectivity towards users with high popularity and the "ordinary users" tend to directly follow the "popular ones" to get the information faster, instead of awaiting the retweets from their current friends.

Gross *et al.* [11] have spotted complex patterns during the evolution of the adaptive network through the healthy, the oscillatory, the bistable and the endemic state. Extensions of Gross's analysis are presented in [19–25]. Instead of a discrete-time model with a unique re-wiring rate in [11, 22], here, we present two continuous-time models, the continuous-time **A**daptive **I**nformation **D**iffusion (**AID**) and the **A**daptive **S**usceptible-**I**nfected-**S**usceptible (**ASIS**) model, with separate link breaking and creating rates. The two seemingly similar epidemic models, both representing real-world appearances but with opposite topology dynamics, surprisingly, exhibit a completely different stability of the metastable state. Moreover, the two models possess a different scaling of the epidemic threshold, while the properties of the metastable topologies show similar, but phase rotated shapes. Interestingly, our analysis does not *resort to mean-field approximations*, taking into account the topological and epidemic variations of the nodes.

The *epidemic* (*information*) *dynamic* in the two models is based on the standard **S**usceptible-**I**nfected-**S**usceptible (**SIS**) epidemic process [26]. We describe the ASIS process, while the terminology for the AID model is given in brackets. The *epidemic* (*information possession*) state of node i in a network G with N nodes is specified by a Bernoulli random variable $X_i(t) \in \{0, 1\}$: $X_i(t) = 1$, if node i is *infected* (*posses the information*) and $X_i(t) = 0$, otherwise. At time t, a node i is infected (posses the in-

* S.Trajanovski@tudelft.nl

† the research was done while D. G. was with the Institute of Information Science, Beijing Jiaotong University, Beijing, P. R. China and during his research visit at Delft University of Technology, The Netherlands.

formation) with probability $\Pr[X_i(t)=1]$. The *epidemic* (*information*) *spreading process* from an infected (information possessing) node to its *healthy* (*information-less*) neighbors is a Poisson process with rate β. Only when node i is infected (has the information), it can infect (share the information) with the direct neighbors with rate β. In an online social network, a user can obtain the information via different sources (e.g., the "social reinforcement" effect [27, 28]) that are not necessarily related to the network, which is modeled by the self-infection rate ε. An infected (information possessing) node *is cured* (*releases the information*) with a Poisson rate δ. The *exact* governing SIS equation for the *infection* (*information possessing*) *probability* of node i, is

$$\frac{d}{dt}E[X_i] = E\left[(-\delta+\varepsilon)X_i + (1-X_i)\beta\sum_{j=1}^{N} a_{ij}X_j\right]. \tag{1}$$

The *topology dynamics* in ASIS and AID, are opposite. In both models, two Poisson processes, the *link-breaking* and *link-creating* with rates ζ and ξ respectively, change the network's topology. In AID, the link-creating process establishes a link between a node pair (i,j), when exactly one node i or j has the information. The link-breaking process removes an existing link between a node pair (i,j), when both i and j do not possess the information, and if there was no link in the original network ($a_{ij}(0)=0$). The **AID** governing equation for the link existence probability $E[a_{ij}(t)] = \Pr[a_{ij}(t)=1]$ is, for $i \neq j$, is

$$\begin{aligned}\frac{d}{dt}E[a_{ij}] =& (1-a_{ij}(0))E\Big[-\zeta a_{ij}(1-X_i)(1-X_j) \\ &+ \xi(1-a_{ij})(X_i-X_j)^2\Big].\end{aligned} \tag{2}$$

As initial graph, we confine ourselves to the empty graph with N nodes and no links ($a_{ij}(0)=0$ for $i\neq j$). The right-hand side of (2) consists of two opposing processes: (a) while either node i or j (but not both) possesses the information, the link between node i and j is created with rate ξ, in this way modeling the tendency for the information-less nodes to obtain the information faster. This link creating process is applicable to information diffusion in online social networks, where friendship and follower links can be changed adaptively; (b) if two adjacent nodes i and j do not have the information, the link between them is broken with rate ζ, due to the absence of incentives of maintaining a link between the information-less nodes. In the case that both node i and j have the information (i.e. $X_i = X_j = 1$), the link is preserved, i.e. $\frac{dE[a_{ij}]}{dt} = 0$. Hence, the link dynamics in (2) tends to increase the degree of a node with information and to decrease the degree of a node without information. For convenience, we denote the *effective information expiring* rate by $\delta^* = \delta - \varepsilon$. By expressing the time in units of δ^*, the model parameters in (1) and (2) can be reduced to the effective information spreading rate $\tau = \frac{\beta}{\delta^*}$, the effective link breaking rate $\omega = \frac{\zeta}{\xi}$ and a choice of either ξ, β or ζ. Just as the SIS process on a fixed graph, the AID process is Markovian [29] with the overall-healthy state (or absorbing state) as steady-state. The relevant physical behavior happens in the metastable state in which the system (SIS process and network) above the epidemic threshold [30] τ_c remains for a long time [26, 31].

We verify that the **AID** model is realistic by using data from Facebook - the most famous social network nowadays. FIG. 1 shows that the AID model is realistic, by verifying Facebook wall posts [32] from the New Orleans area for the last three months [33] of 2008. The rates in the AID model are extracted [34] from the data and the process is detailed in the supplementary material. Subsequently, the prevalence obtained from the AID model and from Facebook data is compared in FIG. 1, illustrating a good fit.

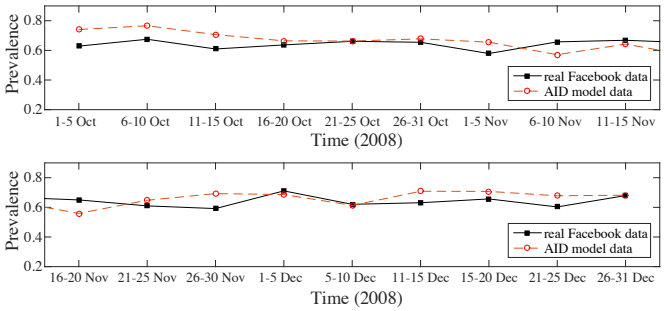

FIG. 1. (Color online) The prevalence of the AID model and the real Facebook data [32] from the New Orleans region (USA) for the last three months of 2008. A good fit is obtained.

In **ASIS** [35], the topology changes in an opposite way: (a) while either node i or j (but not both) is infected, the link between node i and j is removed with rate ζ in order to protect the susceptible node from infection; (b) while both node i and j are susceptible, a link is created between them with rate ξ. For **ASIS**, in the case that both node i and j are infected (i.e. $X_i = X_j = 1$), the link is preserved, whose link dynamic, opposite to (2), is

$$\begin{aligned}\frac{d}{dt}E[a_{ij}] =& a_{ij}(0)\,E\Big[-\zeta a_{ij}(X_i-X_j)^2 \\ &+ \xi(1-a_{ij})(1-X_i)(1-X_j)\Big].\end{aligned} \tag{3}$$

The aim of this paper is to report a striking difference that emerges from the two seemingly "similar" models, AID and ASIS, that both reflect realistic physical phenomena. Both models build upon the SIS epidemic model (1), but adaptively change the topology in opposite ways given in (2) and (3) for AID and ASIS, respectively. The factors $-\zeta a_{ij}$ and $\xi(1-a_{ij})$ multiply $(1-X_i)(1-X_j)$ and $(X_i-X_j)^2$, respectively, for the AID model in (2), while the order of multiplication for the same factors is reverse in the ASIS model in (3). Most importantly, the AID model shows instability and non-existence of the

metastable state for some regions of τ and ω, which is not the case for the ASIS model. The characteristic differences between ASIS and AID are summarized in Table I. We further proceed to explain those differences.

TABLE I. A comparison of the adaptive models.

property/model	ASIS	AID
metastable state	always stable	unstable (τ, ω) regions
threshold $\tau_c(\omega)$	linear	(mostly) constant
topological metrics	"half-elliptical"	rotated "half-elliptical"

Without resorting to any mean-field approximation, we provide exact expressions for the fraction of infected nodes and the epidemic threshold for both models. These relations, although not closed-form expressions, due to the existence of probabilistic and variance terms, provide exact solutions and more interestingly, can explain the existence and stability of the number of infected nodes in the metastable state for both AID and ASIS. The key observation, that the same correlation terms as $E[a_{ij}X_iX_j]$ appear in (1) and in both (2) and (3), led to the explicit relations of the *prevalence*, the fraction of information possessing/infected nodes. We denote by $Z^* = \frac{1}{N}\sum_{j=1}^{N} X_j^*$ the prevalence and the average metastable state or maximal prevalence by $y = E[Z^*]$ in a graph with N nodes. Interestingly, it holds [36]: $\mathrm{Var}[Z^*] < E[Z^*] \leq y \leq 1$. We also denote $T(N) = \frac{E\left[\sum_{i=1}^{N} d_i^*(1-X_i^*)\right]}{N^2}$, which is bounded by

$$0 \leq T(N) \leq \frac{E\left[\sum_{j=1}^{N} d_j^*\right]}{N^2} = \frac{E[2L^*]}{N^2} \leq \frac{N(N-1)}{N^2} < 1.$$

For the **AID model**, we have [37]

$$y = \frac{1}{2}\left(1 + \frac{\omega - 2}{2\tau N}\right)\left(1 \pm \sqrt{1 - \frac{4\mathrm{Var}[Z^*] + 2\omega T(N)}{\left(1 + \frac{\omega-2}{2N\tau}\right)^2}}\right), \tag{4}$$

where $\mathrm{Var}[Z^*]$ and d_j^* denote the variance of the prevalence and the degree of node j, respectively. A key observation from (4), leading to the **non-existence** of the metastable state for AID in some parameter regime, is the possibility that the argument under the square root is negative! Indeed, let us consider a large network size, where $N \to \infty$, so that (4) simplifies to

$$y = \frac{1}{2}\left(1 \pm \sqrt{1 - \left(2\omega T_\infty + 4\mathrm{Var}[Z^*]\right)}\right). \tag{5}$$

Eq. (5) shows that the metastable state does not exist for AID, if $4\mathrm{Var}[Z^*] + 2\omega T_\infty > 1$, and, hence,

$$\mathrm{Var}[Z^*] > \frac{1}{4}$$

is sufficient for the non-existence of the metastable state in AID. Moreover, (5) leads to an upper bound for the link-breaking rate ω:

$$\omega \leq \frac{1 - 4\mathrm{Var}[Z^*]}{2T_\infty} \leq \frac{1}{2T_\infty},$$

otherwise there will not be a metastable state solution.

The consequences of (5) are confirmed by extensive simulations. There are regions for (τ, ω), where the metastable state does not exist, as demonstrated in FIGS. 2a and 2b. The **instability area** exhibits a "sand-clock" shape: it is wider close to the center of the coordinated system, further narrows and then widens again for higher τ and ω. The instability area in AID finally vanishes for high enough τ and ω. Finally, as a side note, we find that there are **regions of instability** even in a more general model from our, where the infection rates change during time [38].

The **ASIS** metastable state prevalence is [37]

$$y = \left(1 - \frac{1}{2N} + \frac{\omega^* - \frac{1}{2}}{\tau N}\right) \times \left(1 \pm \sqrt{1 - \frac{1 - \frac{1}{N} + \mathrm{Var}[Z^*] - T(N)}{\left(1 - \frac{1}{2N} + \frac{\omega^* - \frac{1}{2}}{\tau N}\right)^2}}\right), \tag{6}$$

where the value under the square root in (6) is always positive. Hence, the metastable state always exists [35] and is given by (7) with sign "-". The prevalence y as a function of τ is shown in FIG. 2c. For $N \to \infty$, (6) boils down to

$$y = 1 \pm \sqrt{T_\infty - \mathrm{Var}[Z^*]}. \tag{7}$$

In contrast with the AID model, there is in (7) no constraint on ω for the ASIS metastable state.

For a combination of $(\beta, \delta, \zeta, \xi)$ with relatively higher link breaking rate than the creating rate and "small" spreading rate in the AID model, a small portion of nodes obtains the information, which does not have a potential (the spreading rate is small and breaking rate relatively big) to stay long nor can be considered as a metastable state. Consequently, in such a combination, multiple and sharp changes, both epidemically and topologically, are visualized in FIG. 3a. In the other case of a stable combination, there is a critical mass of links and information-possessing nodes and although there are time changes, the forces of the epidemics reach an equilibrium (e.g, one link is broken, but another is created), which represents the metastable state as shown in FIG. 3b.

The epidemic thresholds can be determined from the equations of both AID and ASIS [37]. Surprisingly, the threshold is linear in ω only for **ASIS**,

$$\tau_c(\omega; \xi) = \frac{2\omega - 1}{N\left(h_{\mathrm{ASIS}}(\omega; \xi) - 2 + \frac{1}{N}\right)}, \tag{8}$$

where $1 \leq h_{\mathrm{ASIS}}(\omega; \xi) \leq 2 + \frac{1}{N}\left(\frac{1}{a} - 1\right)$ and $a = \left.\frac{\partial \tau_c(\omega;\xi)}{\partial \omega}\right|_{\omega \to \infty}$ is almost a constant. The function $h_{\mathrm{ASIS}}(\omega; \xi)$ is a positive, slowly varying, obeying $h_{\mathrm{ASIS}}\left(\frac{1}{2}; \xi\right) = 2 - \frac{1}{N}$ for the ASIS model, for all $\omega > 0$.

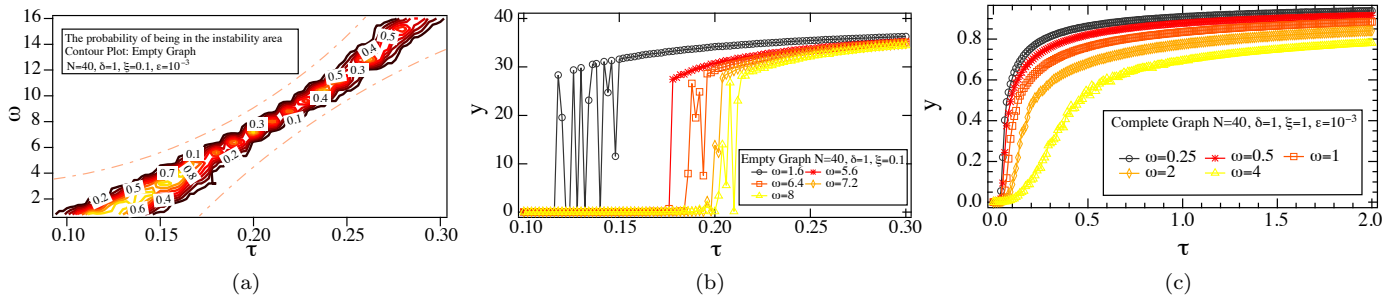

FIG. 2. (Color online) (a) Instability region for the AID model. (b) The prevalence y in the AID model. (c) The prevalence y the ASIS model. (a) and (b) demonstrate the instability in AID. (c) demonstrates the stability in ASIS.

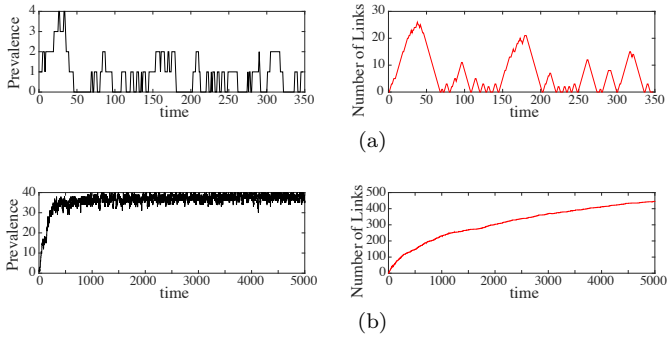

FIG. 3. (Color online) The numbers of links and infected nodes as functions of consecutive time moments in the AID model for $N = 40$, $\zeta = 0.32$, $\xi = 0.1$, $\delta = 1$, $\varepsilon = 10^{-3}$ and different spreading rates β. (a) $\beta = 0.152$; (b) $\beta = 1.0$. The points of instability/stability are in accordance to FIG. 2a.

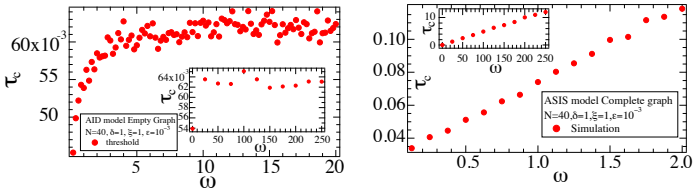

FIG. 4. (Color online) Threshold τ_c versus effective link-breaking rate ω for $N = 40$ (the inset: large range of ω). (a) AID model; (b) ASIS model.

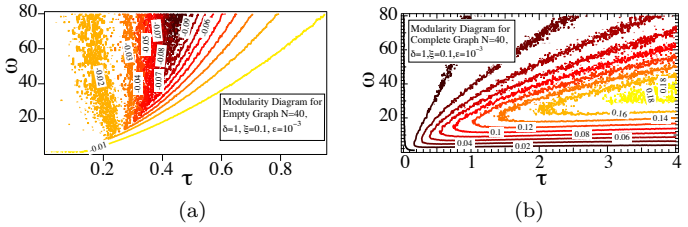

FIG. 5. (Color online) Modularity in (τ, ω)-plane in the stable region for $\xi = 0.1$. (a) AID model; (b) ASIS model.

For **AID**, on the other hand, the information threshold is the quotient of two linear functions, that approaches a constant for large ω,

$$\tau_c(\omega;\xi) = \frac{\omega - 2}{2N\left(h_{\rm AID}(\omega;\xi) - 1\right)}, \tag{9}$$

where $h_{\rm AID}(\omega;\xi) \leq 1 + \max\{1, 1 + \frac{\omega-2}{2Na}\}$ and $a = \lim_{\omega\to\infty} \frac{\partial h_{\rm AID}(\omega;\xi)}{\partial\omega}$ is almost a constant. For $\omega > 2$, the function $h_{\rm AID}(\omega;\xi)$ is almost linear in ω, obeying $h_{\rm AID}(2;\xi) = 1$ for the AID model.

The simulations shown in FIG. 4b indicate that $\tau_c(\omega;\xi)$ increases about linearly in ω, confirming (8) for the ASIS model, while FIG. 4a, for the AID model, demonstrate that the epidemic threshold is quotient of two linear functions in ω, and almost constant for large ω. Finally, a noisy epidemic threshold in FIG. 4a is a fingerprint of the instability in the AID model.

FIG. 5 shows, as a contour plot in the (τ, ω)-plane, the modularity value of the networks in the metastable for both ASIS and AID (where stable). The contour lines resemble roughly concentric half ellipses, for the effective infection rate τ well above the epidemic threshold where the epidemic is active in the metastable state. A remarkable observation is that, for a fixed effective infection rate τ, there are two different values for ω reaching the same value of the metric, each representing the regimes of very small or very high effective link-breaking rates ω. The "half-elliptical" contour lines of the modularity in ASIS and AID only differ in two aspects: (i) the order of the contour lines - "the inner contour" lines show higher modularity in ASIS, and lower in AID; (ii) they are rotated from one another, although the shape is surprisingly similar. In the (τ, ω)-plane, the instability area, which has "sand-clock" shape (FIG. 2a), exists only for the AID model, is just bellow the "half-ellipses" extremal node, looks like their "natural extension" and is close to the center of the coordinate system.

The *metastable state* (where it exists) of the AID model is a random graph, while the metastable state in the ASIS model is a graph with two separated components that are loosely connected, each representing the susceptible (close to complete graph) and infected nodes (random

graph). In the absolute *stable state* in both ASIS and AID models all nodes are susceptible. However, the final stable state topology in AID is an empty graph, while it is a complete graph in ASIS. The metastable states are physically more interesting and those states are the focuses of this paper.

Summarizing, our analysis of the adaptive epidemic models ASIS and AID, with opposite topology dynamic, leads to the following contributions:

1. In the metastable state, there is a "sand-clock" shape area of instability only for the AID model. The ASIS metastable state always exists.

2. The AID epidemic threshold τ_c is almost constant in the effective link-breaking rate ω, while $\tau_c(\omega)$ linearly increases with ω for ASIS.

3. In the (τ, ω)-plane, topological metrics of both adaptive epidemic models exhibit concentric half-ellipses. The ASIS and AID models differ in the order of the ellipses and the rotation.

4. By extracting the model rates (detailed in the supplementary material), we validate the AID model with data [32] from Facebook - the most famous social network nowadays.

Acknowledgement. This work was partially funded by the European project CONGAS (Grant FP7-ICT-2011-8-317672). D. Guo was supported in part by the National Basic Research Program of China (973 Program) under Grant No. 2012CB315801, and in part by the National Natural Science Foundation of China (NSFC) under Grant No. 61170290 and Grant No. 61222213.

[1] M. Newman, *Networks: An Introduction* (OUP, 2010).
[2] P. Van Mieghem, *Graph Spectra for Complex Networks* (Cambridge Univ. Press, UK, 2011).
[3] P. Van Mieghem, *Performance Analysis of Complex Networks and Systems* (Cambridge Univ. Press, UK, 2014).
[4] S. V. Buldyrev, R. Parshani, G. Paul, H. E. Stanley, and S. Havlin, Nature **464**, 1025 (2010).
[5] R. Pastor-Satorras and A. Vespignani, Phys. Rev. Lett. **86**, 3200 (2001).
[6] P. Van Mieghem, Computing **93**, 147 (2011).
[7] S. H. Strogatz, Nature **410**, 268 (2001).
[8] T. House, J. R. Soc. Interf. **8**, 909 (2011).
[9] S. Fortunato and C. Castellano, Physics Today **65**, 74+ (2012), 1210.2426.
[10] Q. Li, L. Braunstein, H. Wang, J. Shao, H. Stanley, and S. Havlin, Journal of Statistical Physics **151**, 92 (2013).
[11] T. Gross, C. J. D. D'Lima, and B. Blasius, Phys. Rev. Lett. **96**, 208701 (2006).
[12] I. B. Schwartz and L. B. Shaw, Physics **3**, 17 (2010).
[13] S. Funk, S. Salathé, and V. A. A. Jansen, J. R. Soc. Interf. **7**, 1247 (2010).
[14] T. Gross and B. Blasius, J. R. Soc. Interf. **5**, 259 (2008).
[15] E. Volz and L. A. Meyers, J. R. Soc. Interf. **6**, 233 (2009).
[16] R. Pastor-Satorras, C. Castellano, P. Van Mieghem, and A. Vespignani, arXiv (*submitted to Review of Modern Physics*) (2014), http://arxiv.org/abs/1408.2701.
[17] D. Antoniades and C. Dovrolis, arXiv **abs/1309.6001** (2014).
[18] S. A. Myers and J. Leskovec, in *Proc. of WWW* (ACM, Seoul, Korea, 2014) pp. 913–924.
[19] V. Marceau, P.-A. Noël, L. Hébert-Dufresne, A. Allard, and L. J. Dubé, Phys. Rev. E **82**, 036116 (2010).
[20] D. H. Zanette and S. Risau-Gusmán, Journal of Biological Physics **34**, 135 (2008).
[21] C. Lagorio, M. Dickison, F. Vazquez, L. A. Braunstein, P. A. Macri, M. V. Migueles, S. Havlin, and H. E. Stanley, Phys. Rev. E **83**, 026102 (2011).
[22] L. D. Valdez, P. A. Macri, and L. A. Braunstein, Phys. Rev. E **85**, 036108 (2012).
[23] I. Tunc, M. S. Shkarayev, and L. Shaw, J. Stat. Phys. **151**, 355 (2013).
[24] S. Wieland, T. Aquino, and A. Nunes, EPL (Europhysics Letters) **97**, 18003 (2012).
[25] T. Rogers, W. Clifford-Brown, C. Mills, and T. Galla, Journal of Statistical Mechanics: Theory and Experiment **2012**, P08018 (2012).
[26] P. Van Mieghem, J. Omić, and R. Kooij, IEEE/ACM Transactions on Networking **17**, 1 (2009).
[27] A. L. Hill, D. G. Rand, M. A. Nowak, and N. A. Christakis, PLoS Comput Biol **6**, e1000968 (2010).
[28] D. Centola, Science **329**, 1194 (2010).
[29] We can enumerate the (huge) state space. From any state, there is a uniquely defined transition to another state with constant rate.
[30] For $\tau < \tau_c$, node j is almost always healthy, $X_j \to 0$, and the link dynamics (2) show that the metastable topology is close to the original graph.
[31] P. Van Mieghem, arXiv abs/1310.3980 (2013).
[32] B. Viswanath, A. Mislove, M. Cha, and K. P. Gummadi, in *Proc. of the 2nd ACM SIGCOMM Workshop on Social Networks (WOSN)* (2009).
[33] After the major redesign of Facebook [32], allowing users to more easily see friends' posts (articles) on its own wall.
[34] The period of 3 months has been divided equally in chunks of 5 days. The rates β, δ, ε, ζ and ξ have been extracted from the data. Details are given in the supplementary material.
[35] D. Guo, S. Trajanovski, R. van de Bovenkamp, H. Wang, and P. Van Mieghem, Phys. Rev. E **88**, 042802 (2013).
[36] Due to Cauchy-Schwarz inequality, we have $(\sum_{j=1}^N X_j)^2 \leq N(\sum_{j=1}^N X_j^2) = N(\sum_{j=1}^N X_j)$, because $X_j \in \{0,1\}$. Now, we can apply this into $\mathrm{Var}[Z^*] = E[Z^2] - (E[Z])^2 \leq E[Z^2] = \frac{1}{N^2}E[(\sum_{j=1}^N X_j)^2] \leq \frac{1}{N^2}E[N\sum_{j=1}^N X_j] = \frac{1}{N}E[\sum_{j=1}^N X_j] = E[Z] \leq 1$.
[37] The derivations are given in the supplementary material.
[38] This is a case in the model of Huang *et al.* [39] for time-changing, activity dependent infection rates. To not break the flow of the paper, more details are given in the supplementary material.
[39] J. Huang, C. Li, W.-Q. Wang, H.-W. Shen, G. Li, and X.-Q. Cheng, Scientific Reports **4**, 5334 (2014).

Supplementary material

I. SCHEMATIC VISUALIZATION OF THE MODELS

The link state changing for both models based on the viral states of a pair of nodes is visualized in FIG. 1. For the AID model, a link is created between a pair of nodes if exactly one node is infected (I) and one is susceptible (S), while an existing link is broken between two susceptible (S) nodes (FIG. 1a). On the other hand, for the ASIS model an existing link is broken between a pair of exactly one susceptible (S) and one infected node (I), while a new link is created between two susceptible (S) nodes (FIG. 1b).

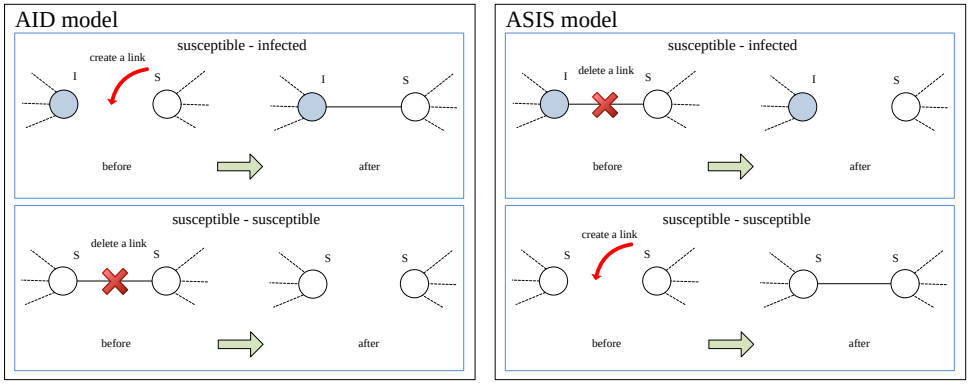

(a) (b)

FIG. 1. (Color online) Link state changing process based on the viral states of a pair of nodes. (a) AID model. (b) ASIS model.

II. AID MODEL

A. Rates extraction from New Orleans Facebook data [1]

TABLE I. Rates for the AID model (on 4 decimal places).

period (2008)	ε	β	δ	$\zeta \times 10^{-4}$	$\xi \times 10^{-4}$	Data prevalence
Oct 1-5	0.0105	0.6809	0.5873	2.3666	2.8165	0.6288
Oct 6-10	0.0101	0.6970	0.5565	1.7692	2.4906	0.6750
Oct 11-15	0.0096	0.6823	0.5990	2.4365	2.6906	0.6095
Oct 16-20	0.0087	0.6932	0.5795	2.2100	2.5333	0.6368
Oct 21-25	0.0093	0.6958	0.5627	1.7615	2.3642	0.6611
Oct 26-31	0.0089	0.7103	0.5639	1.7355	2.2563	0.6546
Nov 1-5	0.0100	0.6912	0.6253	2.6540	2.5270	0.5789
Nov 6-10	0.0080	0.6923	0.5752	1.7662	2.3467	0.6573
Nov 11-15	0.0085	0.7157	0.5576	1.5625	2.1799	0.6682
Nov 16-20	0.0072	0.7052	0.5515	1.7317	2.1085	0.6502
Nov 21-25	0.0099	0.6929	0.5921	2.1168	2.1916	0.6099
Nov 26-30	0.0114	0.6766	0.6204	2.3428	2.4107	0.5917
Dec 1-5	0.0101	0.7110	0.5357	1.1696	1.8996	0.7111
Dec 6-10	0.0100	0.6962	0.5788	1.8217	2.0041	0.6205
Dec 11-15	0.0122	0.6975	0.5804	1.7305	1.9855	0.6311
Dec 16-20	0.0127	0.7109	0.5549	1.4903	1.9097	0.6568
Dec 21-25	0.0112	0.7229	0.6071	1.9511	2.0876	0.6028
Dec 26-31	0.0115	0.7145	0.5558	1.2761	1.8154	0.6794

The data of the last 3 months has been divided into chunks of 5 days. The spreading rate β, curing rate δ, self-infection rate ε, link-breaking rate ζ and link-creating rate ξ are obtained as following.

The self-infection rate ε is proportional to the number of users who posted on their own walls in a given time-chunk, while the spreading rate β is proportional to those who posted others during this period. The curing (recovery or information expiration) rate δ is proportional to those who were infected (i.e. receive the information, posted by others) in the previous time period, but not in the current time chunk. Finally, the link-creating rate ξ is proportional to the number of uniquely established communication between two users in a certain time period, while the link-breaking rate ζ is proportional to these connections that were established during the previous time period, but not in the current one. Finally, the rates are normalized with the time equals to 5 days. The prevalence of the model in the metastable state is obtained after averaging of 50 independent runs.

B. Prevalence y: fraction of information possessing nodes

We transform the link dynamic equation into

$$\begin{aligned}\frac{d}{dt}E[a_{ij}] =& -\zeta E\left[a_{ij}\right] + \xi E\left[X_i\right] + \xi E\left[X_j\right] - 2\xi E\left[X_i X_j\right] \\ &+ (\zeta-\xi)\, E\left[a_{ij}X_i\right] + (\zeta-\xi)\, E\left[a_{ij}X_j\right] + (2\xi-\zeta)\, E\left[a_{ij}X_iX_j\right]\end{aligned}$$

After summing these equations over all $j \neq i$ and using the degree of node i, $d_i = \sum_{j=1}^{N} a_{ij}$ and $a_{ii} = 0$, we arrive at

$$\begin{aligned}\frac{d}{dt}E[d_i] =& -\zeta E\left[d_i\right] + \xi E\left[\left(N-1\right)X_i + \sum_{j=1;j\neq i}^{N} X_j\right] + (\zeta-\xi)\, E\left[d_iX_i + \sum_{j=1}^{N} a_{ij}X_j\right] \\ &- 2\xi E\left[X_i \sum_{j=1;j\neq i}^{N} X_j\right] + (2\xi-\zeta)\, E\left[\sum_{j=1}^{N} a_{ij}X_iX_j\right]\end{aligned}$$

Using

$$\left(N-1\right)X_i + \sum_{j=1;j\neq i}^{N} X_j = \left(N-2\right)X_i + \sum_{j=1}^{N} X_j$$

and

$$X_i \sum_{j=1;j\neq i}^{N} X_j = X_i\left(\sum_{j=1}^{N} X_j - X_i\right) = X_i \sum_{j=1}^{N} X_j - X_i$$

we find

$$\begin{aligned}\frac{d}{dt}E[d_i] =& -\zeta E\left[d_i\right] + \xi E\left[N\cdot X_i + \sum_{j=1}^{N} X_j\right] + (\zeta-\xi)\, E\left[d_iX_i + \sum_{j=1}^{N} a_{ij}X_j\right] \\ &- 2\xi E\left[X_i \sum_{j=1}^{N} X_j\right] + (2\xi-\zeta)\, E\left[\sum_{j=1}^{N} a_{ij}X_iX_j\right] \qquad (1)\end{aligned}$$

Re-writing the governing epidemic expression as

$$E\left[\sum_{j=1}^{N} a_{ij}X_iX_j\right] = -\frac{1}{\beta}\frac{d}{dt}E[X_i] - \frac{1}{\tau}E\left[X_i\right] + E\left[\sum_{j=1}^{N} a_{ij}X_j\right]$$

and substituting into (1) to remove the highest order correlation term, yields

$$\begin{aligned}\frac{d}{dt}E[d_i] =& -\zeta E\left[d_i\right]+\xi E\left[N\cdot X_i+\sum_{j=1}^{N}X_j\right]+\left(\zeta-\xi\right)E\left[d_iX_i+\sum_{j=1}^{N}a_{ij}X_j\right]\\ &-2\xi E\left[X_i\sum_{j=1}^{N}X_j\right]+\left(2\xi-\zeta\right)\left(-\frac{1}{\beta}\frac{d}{dt}E[X_i]-\frac{1}{\tau}E\left[X_i\right]+E\left[\sum_{j=1}^{N}a_{ij}X_j\right]\right)\end{aligned}$$

Using the notation of $\omega=\frac{\zeta}{\xi}$

$$\begin{aligned}\frac{d}{dt}E\left[\frac{d_i}{\zeta}+\frac{\frac{2}{\omega}-1}{\beta}X_i\right] =& -E\left[d_i\right]+\frac{1}{\omega}E\left[N\cdot X_i+\sum_{j=1}^{N}X_j\right]+\left(1-\frac{1}{\omega}\right)E\left[d_iX_i+\sum_{j=1}^{N}a_{ij}X_j\right]\\ &-\frac{2}{\omega}E\left[X_i\sum_{j=1}^{N}X_j\right]+\left(\frac{2}{\omega}-1\right)\left(E\left[\sum_{j=1}^{N}a_{ij}X_j\right]-\frac{1}{\tau}E\left[X_i\right]\right)\\ =& -E\left[d_i+\left(-\frac{N}{\omega}+\frac{\frac{2}{\omega}-1}{\tau}+\left(\frac{1}{\omega}-1\right)d_i\right)X_i\right]\\ &+\frac{1}{\omega}E\left[\sum_{j=1}^{N}X_j\right]-\frac{2}{\omega}E\left[X_i\sum_{j=1}^{N}X_j\right]+\frac{1}{\omega}E\left[\sum_{j=1}^{N}a_{ij}X_j\right]\end{aligned}$$

Using $\sum_{i=1}^{N}d_i=2L$ and summing over all i, we obtain

$$\begin{aligned}\frac{d}{dt}E\left[\frac{2L}{\zeta}+\frac{\left(\frac{2}{\omega}-1\right)}{\beta}\sum_{i=1}^{N}X_i\right] =& -E\left[2L-\frac{1}{\omega}\left(N+\frac{\omega-2}{\tau}\right)\sum_{j=1}^{N}X_j+\left(\frac{1}{\omega}-1\right)\sum_{i=1}^{N}d_iX_i\right]\\ &+\frac{1}{\omega}E\left[N\sum_{j=1}^{N}X_j\right]-\frac{2}{\omega}E\left[\left(\sum_{i=1}^{N}X_i\right)^2\right]+\frac{1}{\omega}E\left[\sum_{j=1}^{N}d_jX_j\right]\\ =& -E\left[2L-\frac{1}{\omega}\left(N+\frac{\omega-2}{\tau}\right)\sum_{j=1}^{N}X_j\right]\\ &+\frac{1}{\omega}E\left[N\sum_{j=1}^{N}X_j\right]-\frac{2}{\omega}E\left[\left(\sum_{i=1}^{N}X_i\right)^2\right]+E\left[\sum_{j=1}^{N}d_jX_j\right]\end{aligned}$$

Simplified, denoting by $Z=\frac{1}{N}\sum_{j=1}^{N}X_j$ the fraction of infected nodes

$$\begin{aligned}\frac{d}{dt}E\left[\frac{2L}{\zeta}+\frac{\left(\frac{2}{\omega}-1\right)N}{\tau\delta^*}Z\right] =& -2E\left[L\right]+\frac{1}{\omega}\left(N+\frac{\omega-2}{\tau}\right)N\cdot E\left[Z\right]\\ &+\frac{N^2}{\omega}E\left[Z\right]-\frac{2N^2}{\omega}E\left[Z^2\right]+E\left[\sum_{j=1}^{N}d_jX_j\right]\\ =& -2E\left[L\right]+\frac{1}{\omega}\left(2N+\frac{\omega-2}{\tau}\right)N\cdot E\left[Z\right]-\frac{2N^2}{\omega}E\left[Z^2\right]+E\left[\sum_{j=1}^{N}d_jX_j\right]\end{aligned}$$

When the derivative at the left-hand side vanishes (in the steady-state or at an extreme value, which we denote by a superscript $*$), we have

$$\left(2N+\frac{\omega-2}{\tau}\right)N\cdot E\left[Z^*\right]-2N^2E\left[(Z^*)^2\right]-\omega E\left[\sum_{i=1}^{N}d_i^*\left(1-X_i^*\right)\right]=0$$

Using $E\left[(Z^*)^2\right] = \mathrm{Var}[Z] + (E[Z^*])^2$ and $y = E[Z^*]$, we arrive at

$$y^2 - \left(1 + \frac{\omega - 2}{2N\tau}\right) y + \left(\mathrm{Var}[Z^*] + \frac{\omega}{2N^2} E\left[\sum_{i=1}^{N} d_i^* (1 - X_i^*)\right]\right) = 0 \tag{2}$$

Solving quadratic equation (2) yields the final expression.

C. Information threshold τ_c

For brevity, we denote by $V = \frac{1}{2} + \frac{\omega-2}{4\tau N}$ and $H = \mathrm{Var}[Z^*] + \frac{\omega}{2N^2} E\left[\sum_{i=1}^{N} d_i^* (1 - X_i^*)\right]$ and equation (2) boils down to $y^2 - 2Vy + H = 0$. For $y > 0$, we have that

$$V = \frac{1}{2}(y + \frac{H}{y})$$

Using the definition of V, we can extract τ as

$$\frac{\omega - 2}{2\tau N} = y + \frac{H}{y} - 1$$
$$\tau = \frac{\omega - 2}{2N(y + \frac{H}{y} - 1)}$$

The epidemic threshold is defined as the largest non-negative value of τ when $y \downarrow 0$, such that

$$\tau_c = \frac{\omega - 2}{2N\left(\lim_{y\downarrow 0} \frac{H}{y} - 1\right)} \tag{3}$$

where $\frac{H}{y} = q(\tau, \omega; \xi)$ is a function of both τ and ω (and ξ)[2], but $\lim_{y\downarrow 0} \frac{H}{y} = q(\tau_c, \omega; \xi) = h_{\mathrm{AID}}(\omega; \xi)$. Thus, we obtain the analytic expression (3) for epidemic threshold. The remainder of the proof consists of demonstrating that $h_{\mathrm{AID}}(\omega; \xi)$ is linearly increasing function in ω.

The two roots of the quadratic equation satisfy $y_1 + y_2 = 2V$ and $y_1 y_2 = H$. Since $H \geq 0$, the roots are either both negative or both positive. Since negative roots have no physical meaning, we must require that $V \geq 0$, which implies, with the definition of V that

$$1 \geq \frac{2 - \omega}{2\tau N}$$
$$\tau \geq \frac{1}{N} - \frac{\omega}{2N}$$

This condition for the effective infection rate τ, which is only confining for $\omega < 2$, can be sharpened. The roots y_1 and y_2 must be real so that the discriminant of the quadratic equation is non-negative, $H \leq V^2$ or $\left(\sqrt{H} - V\right)\left(\sqrt{H} + V\right) \leq 0$. Requiring positive roots so that $0 \leq \sqrt{H} \leq V$, leads, with the definition of V, to

$$\sqrt{H} - \frac{1}{2} \leq \frac{\omega - 2}{4\tau N}$$

If $H \leq \frac{1}{4}$, we arrive at the improved lower bound

$$\frac{1}{2} - \sqrt{H} \geq \frac{2 - \omega}{4\tau N}$$
$$\frac{2 - \omega}{2N(1 - h_{\mathrm{AID}})} = \tau_c \geq \tau^* = \frac{2 - \omega}{2N(1 - 2\sqrt{H})} \tag{4}$$

Since (4) indicates that $\tau^* \leq \tau_c$, there must hold $2\sqrt{H} \leq h_{\mathrm{AID}}(\omega; \xi) < 1$ for $\omega < 2$. A continuity argument requires for $\omega \to 2$ that $\tau_c > 0$ so that $\lim_{\omega\to 2} h_{\mathrm{AID}}(\omega; \xi) = 1$ and $\tau_c(2; \xi) = \frac{1}{2N \left.\frac{\partial h_{\mathrm{AID}}(\omega;\xi)}{\partial \omega}\right|_{\omega=2}}$. For small ω (more link-creation

than link-breaking) there is no a valuable lower bound different from 0, since all the node would anyway receive the information for any τ.

If $\omega \geq 2$ (more link-breaking than link-creation), then there is no confinement for τ. In order to have an epidemic threshold $\tau_c(\omega;\xi) > 0$, there must hold that $h_{\mathrm{AID}}(\omega;\xi) > 1$ for $\omega > 2$. For an extremely high effective link-breaking rate ω, a node that does not possess the information can hardly connect to a node, which posses the information, hence it is natural that the epidemic threshold $\tau_c(\omega;\xi)$ would not increase for high enough $\omega > 2$. Moreover, $\tau_c(\omega;\xi)$ is non-decreasing function, hence $\tau_c(\omega;\xi)$ is almost a constant for high enough ω and $\lim_{\omega\to\infty}\tau_c(\omega;\xi) = const$. The last implies that $h_{\mathrm{AID}}(\omega;\xi)$ is non-decreasing linear function in ω for any $\omega \geq 0$, in which case we deduce from (3) that $\lim_{\omega\to\infty}\frac{\partial h_{\mathrm{AID}}(\omega;\xi)}{\partial\omega} \approx const \neq 0$ and that $h_{\mathrm{AID}}(\omega;\xi) \leq 1 + \frac{\omega-2}{2N\cdot\lim_{\omega\to\infty}\frac{\partial h_{\mathrm{AID}}(\omega;\xi)}{\partial\omega}}$ for all $\omega > 2$.

D. The effects of ε on the instability and the memory effects of the infection rate

We study the effect of different self-infection rates ε for reflecting the "social reinforcement" models as suggested by Hill A. L. *et al.* [3]. The simulations in FIG. 2 confirm that the metastable state may not exists in AID model (i.e. there is also an area of instability) for different ε the same as the theoretical results before in Section II B.

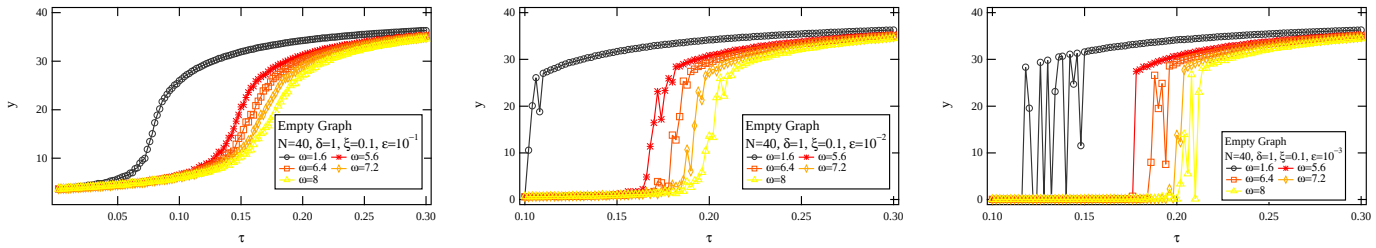

(a) (b) (c)

FIG. 2. (Color online) The instability for the metastable state is present in the AID model. There are differences for the metastable state for different ϵ, but the general claim for the stability of the metastable state holds. (a) $\varepsilon = 10^{-1}$; (b) $\varepsilon = 10^{-2}$; (c) $\varepsilon = 10^{-3}$.

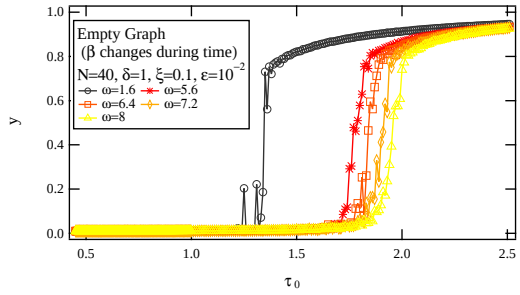

FIG. 3. (Color online) Demonstration of the memory effects and time-changing β according to the model of Huang *et al.* [3]. The metastable state of AID is still unstable for certain parameters.

In order to account the memory and expiration effects, we follow the approach by Huang *et al.* [4], for time-changing infection rates according to the law:

$$\text{Probability of infecting} \propto \beta \propto (t_{\mathrm{cur}} - t_{\mathrm{prev}})^{-0.7}$$

where t_{prev} and t_{cur} are the previous and the current time of infecting. According to FIG. 3, the metastable state may also not exist in this case as in AID model. Finding a theoretical closed-form expression for the prevalence, is infeasible because the infection rates are different (moreover, time changing) and the model cannot be summed up (additively) as we do in Section II B.

III. ASIS MODEL

A. Prevalence y: fraction of infected nodes

We transform the link dynamic equation into

$$\frac{d}{dt}E[a_{ij}] = \xi\left(1 - E\left[a_{ij}\right]\right) - \xi E\left[\left(X_i + X_j\right)\right] - \left(\zeta - \xi\right)E\left[a_{ij}\left(X_i + X_j\right)\right] + \xi E\left[X_i X_j\right] + \left(2\zeta - \xi\right)E\left[a_{ij}X_i X_j\right]$$

After summing these equations over all $j \neq i$ and using the degree of node i, $d_i = \sum_{j=1}^{N} a_{ij}$ and $a_{ii} = 0$, we obtain

$$\frac{d}{dt}E[d_i] = \xi\left(N - 1 - E\left[d_i\right]\right) - \xi E\left[\left(N-1\right)X_i + \sum_{j=1;j\neq i}^{N} X_j\right] - \left(\zeta - \xi\right)E\left[d_i X_i + \sum_{j=1}^{N} a_{ij}X_j\right] + \xi E\left[X_i \sum_{j=1;j\neq i}^{N} X_j\right] + \left(2\zeta - \xi\right)E\left[\sum_{j=1}^{N} a_{ij}X_i X_j\right]$$

Using

$$\left(N-1\right)X_i + \sum_{j=1;j\neq i}^{N} X_j = \left(N-2\right)X_i + \sum_{j=1}^{N} X_j$$

and

$$X_i \sum_{j=1;j\neq i}^{N} X_j = X_i\left(\sum_{j=1}^{N} X_j - X_i\right) = X_i \sum_{j=1}^{N} X_j - X_i$$

we find

$$\frac{d}{dt}E[d_i] = \xi\left(N - 1 - E\left[d_i\right]\right) - \xi E\left[\left(N-1\right)X_i + \sum_{j=1}^{N} X_j\right] - \left(\zeta - \xi\right)E\left[d_i X_i + \sum_{j=1}^{N} a_{ij}X_j\right] + \xi E\left[X_i \sum_{j=1}^{N} X_j\right] + \left(2\zeta - \xi\right)E\left[\sum_{j=1}^{N} a_{ij}X_i X_j\right]$$

Substituting from the governing epidemic expression

$$E\left[\sum_{j=1}^{N} a_{ij}X_i X_j\right] = -\frac{1}{\beta}\frac{d}{dt}E[X_i] - \frac{1}{\tau}E\left[X_i\right] + E\left[\sum_{j=1}^{N} a_{ij}X_j\right]$$

into the above relation to remove the highest order correlation term, yields

$$\frac{d}{dt}E[d_i] = \xi\left(N-1\right) - \xi E\left[d_i\right] - \xi E\left[\left(N - 1 + \frac{\left(2\zeta - \xi\right)}{\tau\xi}\right)X_i\right] - \xi E\left[\sum_{j=1}^{N} X_j\right] - \left(\zeta - \xi\right)E\left[d_i X_i\right] + \xi E\left[X_i \sum_{j=1}^{N} X_j\right] - \frac{\left(2\zeta - \xi\right)}{\beta}\frac{d}{dt}E[X_i] + \zeta E\left[\sum_{j=1}^{N} a_{ij}X_j\right]$$

Rewritten, using $\omega = \frac{\zeta}{\xi}$,

$$\frac{d}{dt}E\left[\frac{d_i}{\xi} + \frac{\left(2\omega - 1\right)}{\beta}X_i\right] = N - 1 - E\left[d_i + \left(N - 1 + \frac{2\omega - 1}{\tau} + \left(\omega - 1\right)d_i\right)X_i\right] - E\left[\sum_{j=1}^{N} X_j\right] + E\left[X_i \sum_{j=1}^{N} X_j\right] + \omega E\left[\sum_{j=1}^{N} a_{ij}X_j\right]$$

Now, we sum over all i, using $\sum_{i=1}^{N} d_i = 2L$, then

$$\frac{d}{dt}E\left[\frac{2L}{\xi}+\frac{(2\omega-1)}{\beta}\sum_{i=1}^{N}X_i\right] = N(N-1) - E\left[2L+\left(N-1+\frac{2\omega-1}{\tau}\right)\sum_{i=1}^{N}X_i+(\omega-1)\sum_{i=1}^{N}d_iX_i\right] - E\left[N\sum_{j=1}^{N}X_j\right]+E\left[\left(\sum_{i=1}^{N}X_i\right)^2\right]+\omega E\left[\sum_{j=1}^{N}d_jX_j\right]$$

Simplified, with $\tilde{t}=\delta^* t$ and the fraction of infected nodes $Z=\frac{1}{N}\sum_{j=1}^{N}X_j$

$$\frac{d}{d\tilde{t}}E\left[\frac{2\delta^* L}{\xi}+\frac{(2\omega-1)N}{\tau}Z\right] = N(N-1) - N\left(2N-1+\frac{2\omega-1}{\tau}\right)E[Z] + N^2E\left[Z^2\right]+E\left[\sum_{i=1}^{N}d_iX_i\right]-E[2L]$$

When the derivative at the left-hand side vanishes (in the steady-state or at an extreme value, which we denote by a superscript $*$) and using $E\left[Z^2\right]=\mathrm{Var}[Z]+(E[Z])^2$ and $y=E[Z^*]$, we arrive at

$$N(N-1)-N\left(2N-1+\frac{2\omega-1}{\tau}\right)y+N^2(y^2+\mathrm{Var}[Z^*])-E\left[\sum_{i=1}^{N}d_i^*(1-X_i^*)\right]=0$$

or

$$y^2-\left(2-\frac{1}{N}+\frac{2\omega-1}{\tau N}\right)y+\left(1-\frac{1}{N}+\mathrm{Var}[Z^*]-\frac{1}{N^2}E\left[\sum_{i=1}^{N}d_i^*(1-X_i^*)\right]\right)=0 \tag{5}$$

Solving quadratic equation (5) gives the final expression.

B. Epidemic threshold τ_c

For simplicity, we denote by $V=1-\frac{1}{2N}+\frac{2\omega-1}{2\tau N}$ and $H=1-\frac{1}{N}+\mathrm{Var}[Z^*]-\frac{1}{N^2}E\left[\sum_{i=1}^{N}d_i^*(1-X_i^*)\right]$ and equation (5) boils down to $y^2-2Vy+H=0$. For $y>0$, we have that

$$V=\frac{1}{2}(y+\frac{H}{y})$$

Using the definition of V, we can extract τ as

$$\frac{2\omega-1}{2\tau N}=\frac{1}{2}(y+\frac{H}{y})-1+\frac{1}{2N}$$
$$\tau=\frac{2\omega-1}{2N\left(\frac{1}{2}\left(y+\frac{H}{y}\right)-1+\frac{1}{2N}\right)}$$

The epidemic threshold is defined as the largest non-negative value of τ when $y\downarrow 0$, such that

$$\tau_c=\frac{2\omega-1}{N\left(\lim_{y\downarrow 0}\frac{H}{y}-2+\frac{1}{N}\right)} \tag{6}$$

where $\frac{H}{y}=q(\tau,\omega;\xi)$ is a function of both τ and ω (and ξ), but $\lim_{y\downarrow 0}\frac{H}{y}=q(\tau_c,\omega;\xi)=h(\omega;\xi)$. Thus, we obtain the analytic expression (6) for epidemic threshold. The remainder of the proof consists of demonstrating that $h(\omega;\xi)$ is a positive, slowly varying function.

The two roots of the quadratic equation satisfy $y_1+y_2=2V$ and $y_1y_2=H$. Since $H\geq 0$, the roots are either both negative or both positive. Since negative roots have no physical meaning, we must require that $V\geq 0$, which implies, with the definition of V that

$$\frac{1-2\omega}{2N\left(1-\frac{1}{2N}\right)}\leq\tau$$

This condition for the effective infection rate τ, which is only confining for $\omega < \frac{1}{2}$, can be sharpened. The roots y_1 and y_2 must be real so that the discriminant of the quadratic equation is non-negative, $H \leq V^2$ or $\left(\sqrt{H} - V\right)\left(\sqrt{H} + V\right) \leq 0$. Requiring positive roots so that $0 \leq \sqrt{H} \leq V$, leads, with the definition of V, to

$$\frac{2\omega - 1}{2N\left(\sqrt{H} + \frac{1}{2N} - 1\right)} \geq \tau$$

Since $\sqrt{H} + \frac{1}{2N} - 1 < 0$, we arrive at the improved lower bound

$$\frac{1 - 2\omega}{2N\left(1 - \frac{1}{2N} - \sqrt{H}\right)} = \tau^* \leq \tau \tag{7}$$

If $\omega \geq \frac{1}{2}$ (more link-breaking than link-creation), then there is no confinement for τ.

Since (7) indicates, for $\omega < \frac{1}{2}$, that $\tau^* \leq \tau_c$, there must hold for $\omega < \frac{1}{2}$ that $2\sqrt{H} \leq h_{\mathrm{ASIS}}(\omega;\xi) < 2 - \frac{1}{N}$. In particular, $h(0;\xi) \geq 1$ because $\tau_c(0;\xi) \geq \frac{1}{N-1}$, the epidemic threshold in SIS epidemics in K_N without link dynamics. More precisely, with $\tau_c(0;\xi) = \frac{1}{N}\left(1 + \frac{c}{\sqrt{N}} + O\left(N^{-1}\right)\right)$, we find

$$h_{\mathrm{ASIS}}(0;\xi) = 1 + \frac{c}{\sqrt{N}} + O\left(N^{-1}\right)$$

A continuity argument requires for $\omega \to \frac{1}{2}$ that $\tau_c > 0$ so that $\lim_{\omega \to \frac{1}{2}} h_{\mathrm{ASIS}}(\omega;\xi) = 2 - \frac{1}{N}$ and $\tau_c\left(\frac{1}{2};\xi\right) = \frac{1}{N \left.\frac{\partial h_{\mathrm{ASIS}}(\omega;\xi)}{\partial \omega}\right|_{\omega=1}}$. For $\omega > \frac{1}{2}$ to have an epidemic threshold $\tau_c(\omega;\xi) > 0$, there must hold that $h_{\mathrm{ASIS}}(\omega;\xi) > 2 - \frac{1}{N}$. For an extremely high effective link-breaking rate ω, an infected node is immediately isolated from the healthy nodes almost surely and cures in isolation so that the epidemic threshold $\tau_c(\omega;\xi)$ is increasing for all $\omega > \frac{1}{2}$ and that $\lim_{\omega\to\infty} \tau_c(\omega;\xi) = \infty$. It is reasonable to assume that $h_{\mathrm{ASIS}}(\omega;\xi)$ is not decreasing in ω for any $\omega \geq 0$, in which case we deduce from (6) that $\lim_{\omega\to\infty} \frac{\partial h_{\mathrm{ASIS}}(\omega;\xi)}{\partial \omega} = 0$ and that $h_{\mathrm{ASIS}}(\omega;\xi) \leq 2 + \frac{1}{N}\left(\frac{1}{\left.\frac{\partial \tau_c(\omega;\xi)}{\partial \omega}\right|_{\omega\to\infty}} - 1\right)$ for all $\omega > \frac{1}{2}$.

C. The effect of self-infection rate ε

For the ASIS model, we also study the effect of different self-infection rates ε for reflecting the chance of being ill due to season/weather conditions, which is considered by Hill *et al.* [3]. The simulations in FIG. 4 show the same as the theoretical results before in Section III A that the metastable state always exists in ASIS model for different ε.

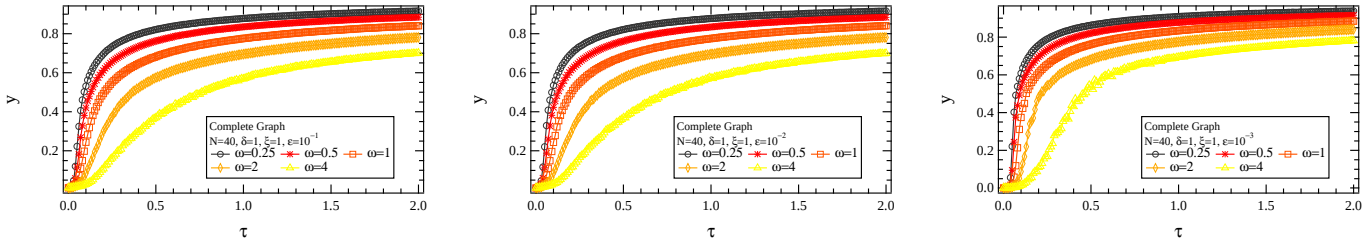

(a) (b) (c)

FIG. 4. (Color online) The metastable state in the ASIS model is always stable. There are differences for the metastable state for different ϵ, but the general claim for the stability of the metastable state holds. (a) $\varepsilon = 10^{-1}$; (b) $\varepsilon = 10^{-2}$; (c) $\varepsilon = 10^{-3}$.

[1] B. Viswanath, A. Mislove, M. Cha, and K. P. Gummadi, in *Proc. of the 2nd ACM SIGCOMM Workshop on Social Networks (WOSN)* (2009).

[2] Besides the two ratios τ and ω, we need the link-creation rate ξ (or β or ζ) to determine the time relation that couples the link dynamics to the epidemic process.
[3] A. L. Hill, D. G. Rand, M. A. Nowak, and N. A. Christakis, PLoS Comput Biol **6**, e1000968 (2010).
[4] J. Huang, C. Li, W.-Q. Wang, H.-W. Shen, G. Li, and X.-Q. Cheng, Scientific Reports **4**, 5334 (2014).